Electronic Supplementary Material (ESI) for Nanoscale.


# Supporting Information

## Tunable fluorescent amino-functionalized $Ti_3C_2T_x$ MXene quantum dots for ultrasensitive $Fe^{3+}$ ion sensing

Zhiwei Wang[a,b], Yuanhang Zhu[a], Yuchen Wu[a,b], Weiyuan Ding[a,b], and Xiuting Li[a,*]

[a]Institute for Advanced Study, Shenzhen University, Shenzhen, 518060, China

[b]Key Laboratory of Optoelectronic Devices and Systems, College of Physics and Optoelectronic Engineering, Shenzhen University, Shenzhen, 518060, China

*Corresponding author: Xiuting Li

E-mail: xiuting.li@szu.edu.cn

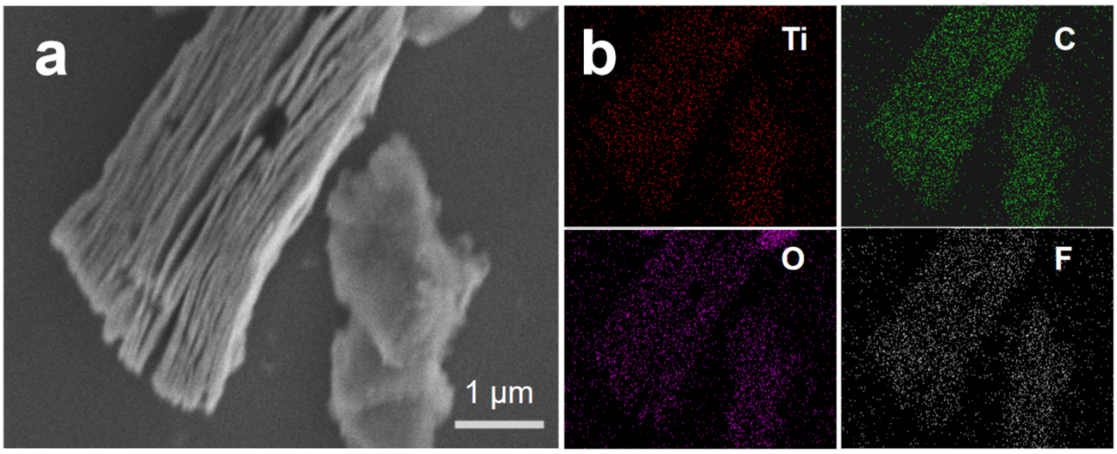


**Figure S1.** (a) SEM image of $Ti_3C_2T_x$ and (b) the corresponding EDS elemental mapping images.

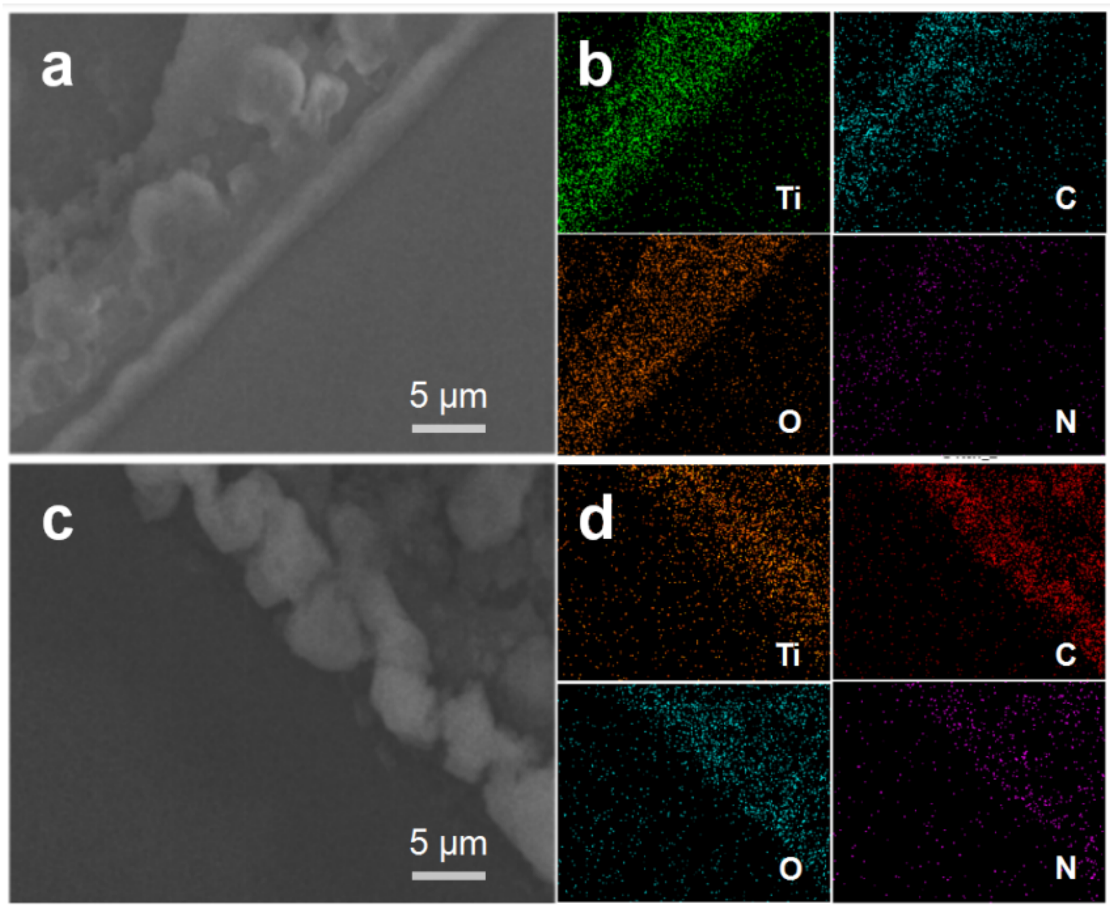


**Figure S2.** (a) SEM image of agglomerated MQDs and (b) the corresponding EDS elemental mapping images. (c) SEM image of agglomerated N-MQDs and (d) the corresponding EDS elemental mapping images.

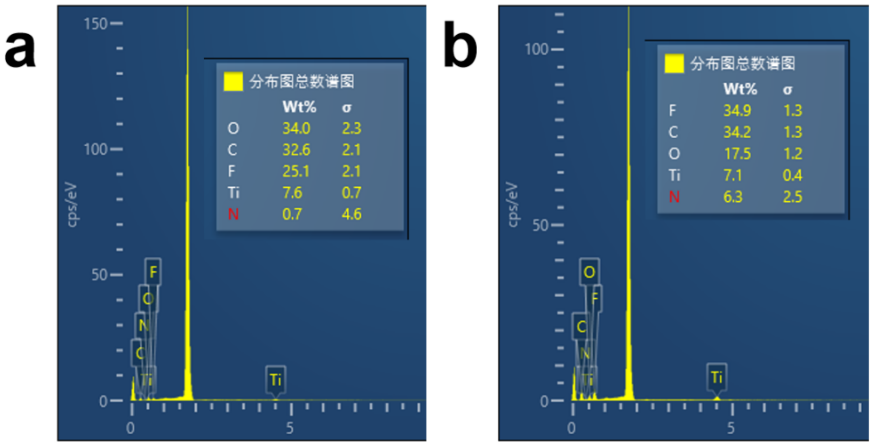


**Figure S3.** SEM-EDS of MQDs and N-MQDs.

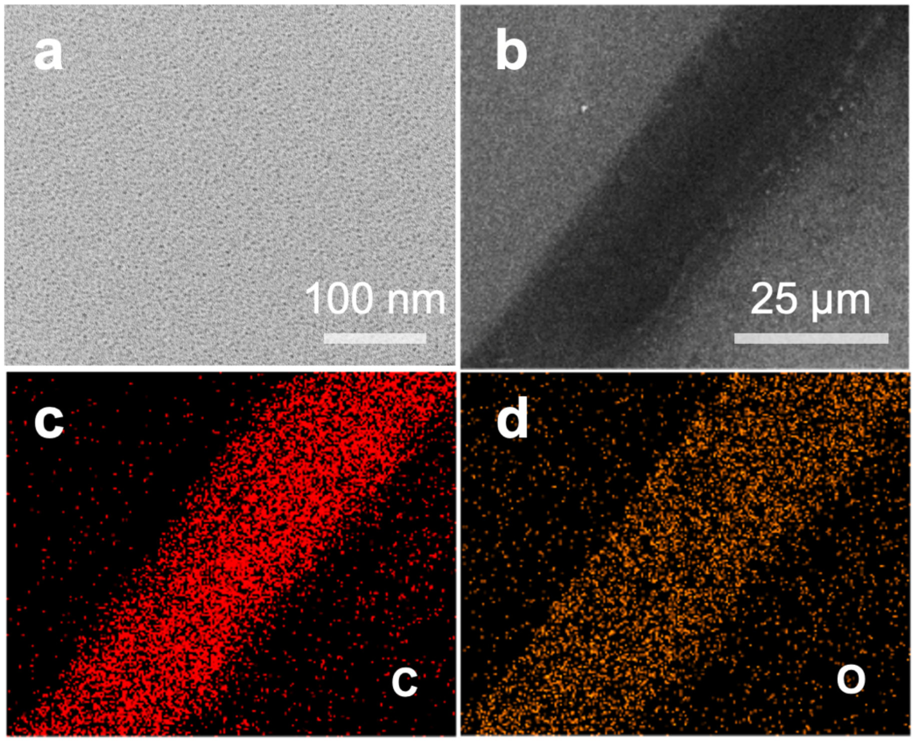


**Figure S4.** (a) TEM image of CQDs and (b) SEM image of agglomerated CQDs and (c), (d) the corresponding EDS elemental mapping images.

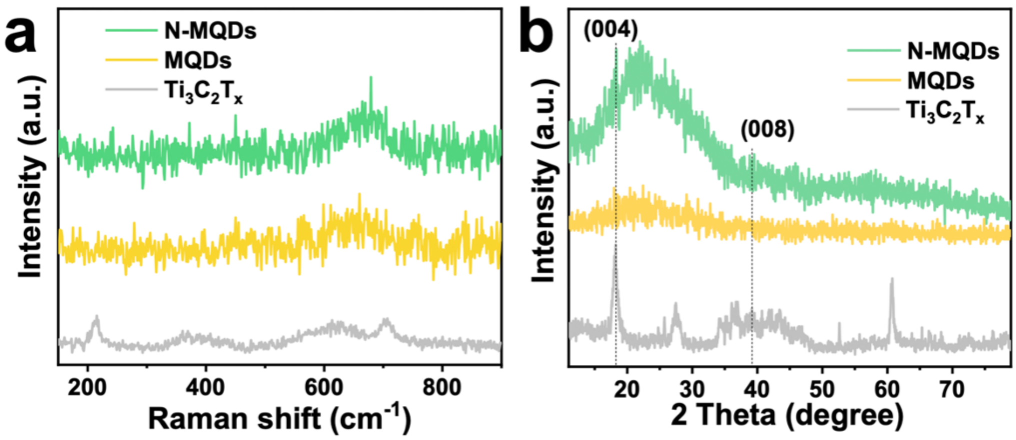


**Figure S5.** (a) Raman spectra and (b) XRD patterns of $Ti_3C_2T_x$, MQDs and N-MQDs.

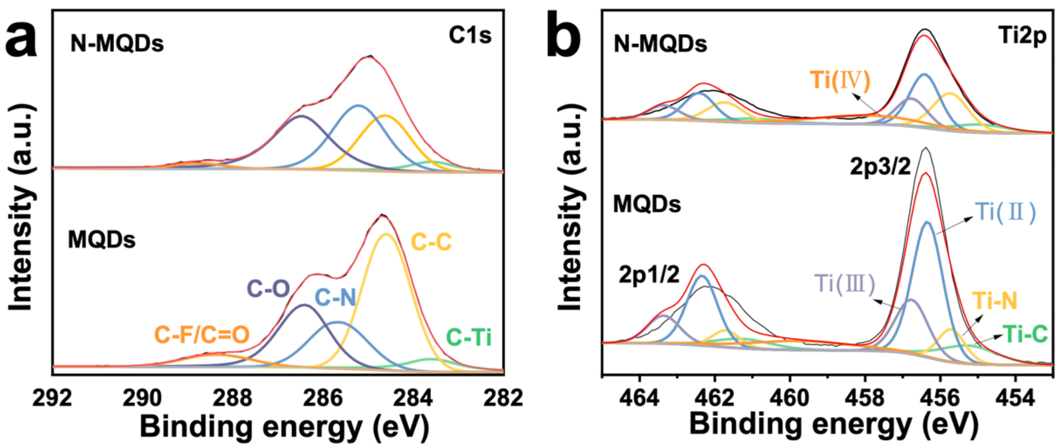


**Figure S6.** High-resolution XPS spectra of (a) C 1s and (b) Ti 2p for MQDs and N-MQDs.

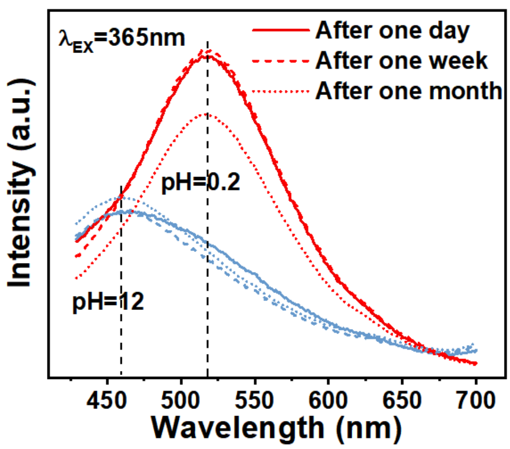


**Figure S7.** PL stability of N-MQDs at the pH of 12 (blue) and 0.2 (red) under the excitation of 365 nm.

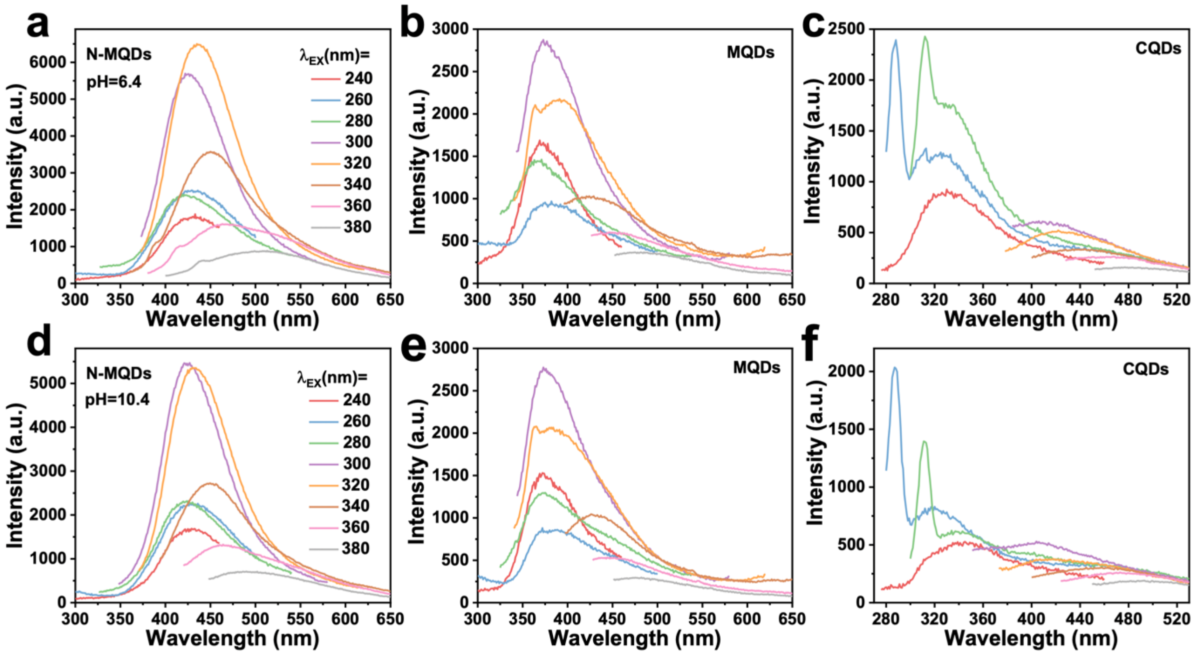


**Figure S8.** PL spectra of different QDs under varying excitation wavelength at the pH of (a-c) 6.4 and (d-f) 10.4.

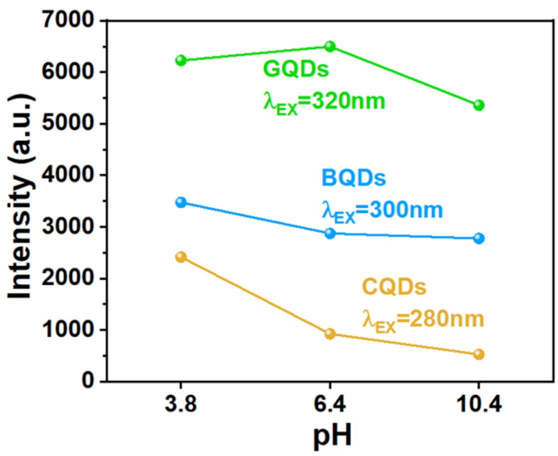


**Figure S9.** The plot of the PL emission peak intensity against the pH for the three different QDs.

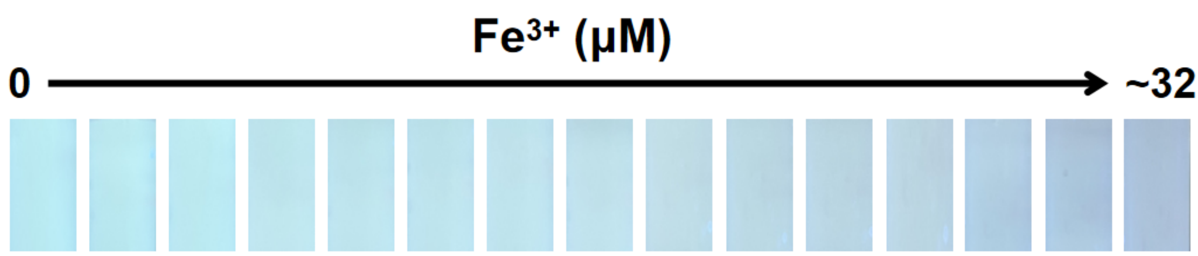


**Figure S10.** Fluorescent photos of the N-MQDs in the presence of $Fe^{3+}$ with different concentration at the pH of 3.8. The photos were taken under a 365 nm UV lamp.

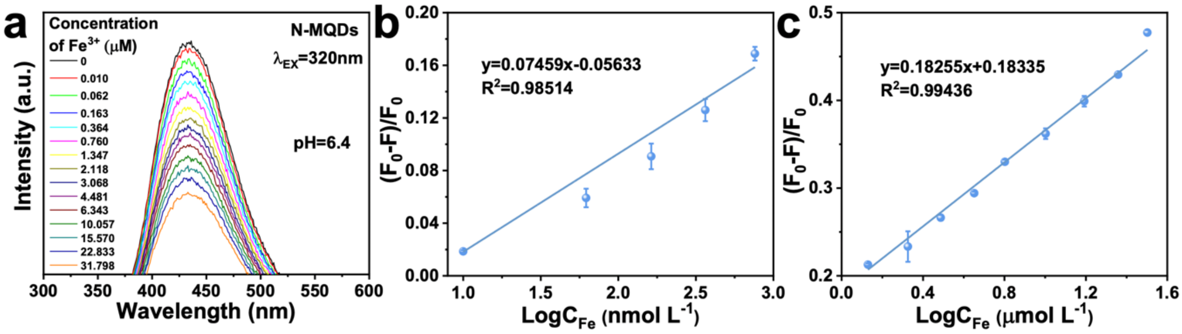


**Figure S11.** (a) PL spectra of the N-MQDs in the presence of $Fe^{3+}$ (0–32 μM) at the pH of 6.4. Linear relationship between $F_0$–$F/F_0$ and the logarithm of $Fe^{3+}$ concentration in the (b) nanomolar range (<1 μM) and (c) micromolar range (<32 μM).

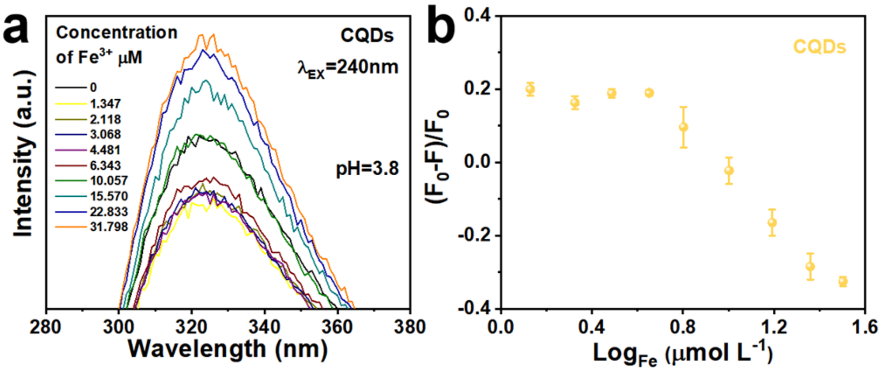


**Figure S12.** (a) CQDs in the presence of $Fe^{3+}$ at the pH of 3.8. (b) Linear relationship between $F_0$–$F/F_0$ and the concentration of $Fe^{3+}$ in the micromolar range (<32 μM) for CQDs.

**Table S1.** Performance comparison of different fluorescent nanoprobes for the detection of $Fe^{3+}$.

| Probe | Detection method | LOD (nM) | Linear range (μM) | Reference |
|---|---|---|---|---|
| $T_3C_2T_x$ QDs | Fluorometry | 310 | 5−1000 | 1 |
| N-$T_3C_2T_x$ QDs | Fluorometry | 2000 | 2−5000 | 2 |
| Graphene QDs | Fluorometry | 20 | 0−1 | 3 |
| Graphene QDs | Fluorometry | 230 | 0.1−20 | 4 |
| S-Graphene QDs | Fluorometry | 4.2 | 0.01−0.7 | 5 |
| Carbon QDs | Fluorometry | 63.4 | 0.37−1500 | 6 |
| Graphene QDs | Fluorometry | 450 | 0−60 | 7 |
| P-Carbon QDs | Fluorometry | 9.5 | 0.02−3 | 8 |
| N, S-Carbon QDs | Fluorometry | 190 | 0.3−70 | 9 |
| B, N, S-Carbon QDs | Fluorometry; colorimetry | 90 | 0.3−546 | 10 |
| N-Carbon QDs | Fluorometry | 520 | 1−250 | 11 |
| N, P-Carbon QDs | Fluorometry | 330 | 1−150 | 12 |
| B, N-Carbon QDs | Fluorometry | 80 | 2−160 | 13 |
| N-Graphene QDs | Fluorometry | 17 | 0−0.125 | 14 |
| N-Carbon QDs | Fluorometry | 100 | 2−20 | 15 |
| F-Carbon QDs | Fluorometry | 10 | 1−100 | 16 |
| N-Graphene QDs | Fluorometry | 63 | 0−80 | 17 |
| Carbon QDs | Fluorometry | 355.4 | 0−1000 | 18 |
| N-Carbon QDs | Fluorometry | 500 | 0−70 | 19 |
| N-Carbon QDs | Fluorometry | 73 | 0.1−4 | 20 |
| Carbon QDs | Fluorometry | 770 | 0−300 | 21 |

| | | | | |
|---|---|---|---|---|
| N, P-Carbon QDs | Fluorometry | 447 | 0−250 | 22 |
| Carbon QDs | Fluorometry | 5230 | 0−500 | 23 |
| N-MQDs | Fluorometry | 2 | 0−32 | This work |

**Table S2.** Results for the determination of $Fe^{3+}$ in tap water, pond water and mineral water samples.

| Samples | Concentration from ICP (nM) | Concentration from the present method (nM) | Recovery (%) |
|---|---|---|---|
| Tap water | 54 | 60 ± 7 | 111 |
| Pond water | 84 | 89 ± 9 | 106 |
| Mineral water | 63 | 70 ± 8 | 111 |

**Table S3.** Results for the determination of $Fe^{3+}$ with spiked concentration in tap water.

| Spiked concentration of $Fe^{3+}$ (nM) | Total $Fe^{3+}$ concentration after addition (nM) | Found (nM) | Recovery (%) |
|---|---|---|---|
| 20 | 74 | 84 ± 4 | 115 |
| 50 | 103 | 109 ± 8 | 106 |
| 100 | 153 | 161 ± 6 | 106 |
| 200 | 252 | 256 ± 3 | 102 |
| 500 | 549 | 554 ± 4 | 101 |

References:


1. Q. Zhang, Y. Sun, M. Liu and Y. Liu, *Nanoscale*, 2020, 12, 1826-1832.
2. Q. Xu, L. Ding, Y. Wen, W. Yang, H. Zhou, X. Chen, J. Street, A. Zhou, W.-J. Ong and N. Li, *Journal of Materials Chemistry C*, 2018, 6, 6360-6369.
3. R. Guo, S. Zhou, Y. Li, X. Li, L. Fan and N. H. Voelcker, *ACS Applied Materials & Interfaces*, 2015, 7, 23958-23966.
4. R. Qiang, W. Sun, K. Hou, Z. Li, J. Zhang, Y. Ding, J. Wang and S. Yang, *ACS Applied Nano Materials*, 2021, 4, 5220-5229.
5. S. Li, Y. Li, J. Cao, J. Zhu, L. Fan and X. Li, *Analytical Chemistry*, 2014, 86, 10201-10207.
6. S. Rajendran, D. V. Ramanaiah, S. Kundu and S. K. Bhunia, *ACS Applied Nano Materials*, 2021, 4, 10931-10942.

7. X. Zhu, Z. Zhang, Z. Xue, C. Huang, Y. Shan, C. Liu, X. Qin, W. Yang, X. Chen and T. Wang, *Analytical Chemistry*, 2017, 89, 12054-12058.
8. G. Kalaiyarasan, J. Joseph and P. Kumar, *ACS Omega*, 2020, 5, 22278-22288.
9. Q. Liu, X. Niu, K. Xie, Y. Yan, B. Ren, R. Liu, Y. Li and L. Li, *ACS Applied Nano Materials*, 2021, 4, 190-197.
10. Y. Liu, W. Duan, W. Song, J. Liu, C. Ren, J. Wu, D. Liu and H. Chen, *ACS Applied Materials & Interfaces*, 2017, 9, 12663-12672.
11. Y. Song, C. Zhu, J. Song, H. Li, D. Du and Y. Lin, *ACS Applied Materials & Interfaces*, 2017, 9, 7399-7405.
12. J. Shangguan, J. Huang, D. He, X. He, K. Wang, R. Ye, X. Yang, T. Qing and J. Tang, *Analytical Chemistry*, 2017, 89, 7477-7484.
13. Y. Zhang, H. Qin, Y. Huang, F. Zhang, H. Liu, H. Liu, Z. J. Wang and R. Li, *Journal of Materials Chemistry B*, 2021, 9, 4654-4662.
14. N. Sohal, S. K. Bhatia, S. Basu and B. Maity, *New Journal of Chemistry*, 2021, 45, 19941-19949.
15. Z. M. S. H. Khan, R. S. Rahman, Shumaila, S. Islam and M. Zulfequar, *Optical Materials*, 2019, 91, 386-395.
16. D. Hong, X. Deng, J. Liang, J. Li, Y. Tao and K. Tan, *Microchemical Journal*, 2019, 151, 104217.
17. Z. Wang, D. Chen, B. Gu, B. Gao, Z. Liu, Y. Yang, Q. Guo, X. Zheng and G. Wang, *Diamond and Related Materials*, 2020, 104, 107749.
18. R. Wang, L. Jiao, X. Zhou, Z. Guo, H. Bian and H. Dai, *Journal of Hazardous Materials*, 2021, 412, 125096.
19. J. Zhu, H. Chu, T. Wang, C. Wang and Y. Wei, *Microchemical Journal*, 2020, 158, 105142.
20. B. Liu, J. Tao, J. Pan, C. Li, F. Li and Y. Zheng, *Optical Materials*, 2021, 113, 110892.
21. L. Zhu, D. Shen, Q. Liu, C. Wu and S. Gu, *Applied Surface Science*, 2021, 565, 150526.
22. S.-R. Zhang, S.-K. Cai, G.-Q. Wang, J.-Z. Cui and C.-Z. Gao, *Journal of Molecular Structure*, 2021, 1246, 131173.
23. S. Ding, Y. Gao, B. Ni and X. Yang, *Inorganic Chemistry Communications*, 2021, 130, 108636.